

CLIMATOLOGY OF THE MARTIAN POLAR REGIONS: THREE MARS YEARS OF CRISM/MARCI OBSERVATIONS OF ATMOSPHERIC CLOUDS AND DUST. A.J. Brown¹ and M. J. Wolff² ¹SETI Institute, 189 N. Bernardo Ave Mountain View, CA 94043, abrown@seti.org, ²Space Science Institute (18970 Cavendish Rd, Brookfield, WI, 53045). Author website: <http://abrown.seti.org>

Introduction: Here we continue the work started in [1,2] to document the dust and ice opacity of the atmosphere in the polar regions for Martian Years 28/29 and 30.

CRISM has been used to map the surface CO₂ and H₂O ice cap springtime recessions for the north and south polar cap [3,4]. Grain size estimates were made of the surface ice, enabling us to constrain models of surface composition for the purposes of modeling the overlying atmosphere.

CRISM has the ability to take ‘gimballed’ observations of the surface as it passes over a target, thus creating what is termed an Emission Phase Function ‘EPF’ measurement (Figure 1) [5]. We report here on our initial investigations of the EPF polar observations and our attempts to model dust and ices suspended in the atmosphere and soil and ice covered surface.

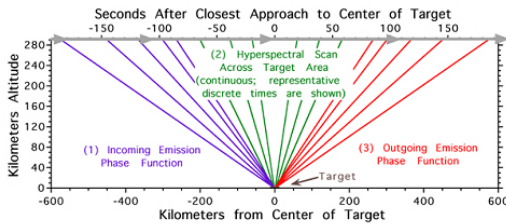


Figure 1. Schematic of a CRISM EPF observation.

Table 1 shows all the CRISM EPF observations poleward of 55°. CRISM is limited to daytime observations and MRO is in a ~250km circular orbit that crosses the equator south to north at 1500 local Mars standard time.

Retrieval Method: We are using the DISORT [6] algorithm to simulate the interaction of the Martian atmosphere and surface with the incident solar radiation with the goal of extracting three parameters: surface Lambert albedo, dust and ice aerosol optical depth. At present, the retrieval is accomplished by fitting a CRISM EPF (in a least-squares sense) at a single wavelength (0.696 micron) – we will be moving to multiple wavelengths in the near future to more effectively discriminate between the dust and water ice atmospheric components.

Computational efficiency is obtained by using the Look-up table approach, where we have pre-computed (millions of) radiative transfer models that span the possible range of optical depth and aerosol values.

Earth DOY	MY/L	EPF	FRT	HRL	HRS	Earth DOY	MY/L	EPF	FRT	HRL	HRS
06-272-298	28(131-125)	21	6	5	1	06-352-5	28(152-159)	8			
298-312	1125-132					006-016	1160-168	9			
312-326	1132-139	10	8	2	13	016-033	1168-176	3		3	1
326-340	1139-146	6	7	1	1	033-044	1176-183	10	6	3	4
340-354	1146-153	15	13	4	7	044-059	1183-192	20	17	1	6
354-07 003	1153-161	20	3	2		059-073	1192-200	8	20	1	5
003-017	1161-168	24	6	2	1	073-086	1200-208	2	14		1
017-031	1168-176	2	1	3	1	086-101	1208-217	25	27		24
031-048	1176-185	11	3	1		101-115	1217-225	17	29	11	12
Northern winter						115-116	1225-234			4	1
---	---	36	1	2	3	132-142	1234-243		36		3
255-269	1312-320	14	7	1		142-156	1243-252	27	42	5	8
269-283	1320-328		2	4	1	156-171	1252-261	3	37	7	2
283-297	1328-335		1	2		171-185	1261-270	12	48	4	1
297-311	1335-344	1	1			185-198	1270-278	124	30	2	2
311-325	1344-351					199-212	1278-286	43	30		
325-339	1351-358					213-225	1286-295	49	137	1	6
339-353	1358-005	9				227-240	1295-303	22	117	2	2
353-08 002	290(5-12)	38				241-255	1303-312		117	4	
08 002-016	112-119	78	9	1		255-269	1312-320	16	66	3	4
016-030	119-25	122	10	3		269-283	1320-328		34	16	4
030-044	125-32	144	8			283-297	1328-335		49	5	13
044-058	132-38	120	18	7		297-311	1335-344		18	8	4
058-072	138-44	159	18	38		311-348	1344-002				
072-086	144-50	9	1			348-00 29(002-012)		61	1	2	
086-100	150-56					08 004-33	1012-026		43	3	
100-114	156-62	50	4	7		033-074	1026-044		39	3	2
114-128	162-69	74	38	16		Southern winter					
128-142	169-75	29	15	2		356-09 001	1177-184		8	2	
142-156	175-81	13	1			019-033	1194-202		14	1	
156-170	181-87	44	12			034-050	1203-211		13	8	16
170-184	187-93	53	17	2		051-067	1214-223		8	4	2
184-198	193-100	43	59	12		069-082	1223-233		46	17	10
198-212	1100-190	59	19	4		083-097	1233-242		31	18	10
212-226	1106-112	22	34	9		098-112	1242-252		28	30	4
226-240	1112-119	46	25	25		113-126	1252-261		16	14	9
240-254	1119-125	47	14	21		128-142	1261-271		37	8	10
254-268	1125-132	22	12	22		143-154	1271-278		14	16	5
268-282	1132-139	32	4	7		162-175	1282-292		15	2	
282-296	1139-146	32	24	14		176-192	1292-302		16	14	12
296-310	1146-153	21	22	11		193-206	1302-310		28	14	17
310-325	1153-160	39	4	17		207-217	1310-317		15	20	5
356-09 012	1177-190	4				223-237	1319-327			41	
Northern winter						Southern winter followed by MRO in safe mode					
193-233	1301-325	2	1	1		TOTAL n=2177 399 1319 252 207					
MRO in safe mode											
10 031-039	30145-49	37	15								

Table 1. Totals of CRISM observations relevant to this study. North polar observations are on the left, and south polar on the right. Counts in italics indicate some missing geometries. Each line corresponds to the two week MRO planning cycle. DOY column gaps are when CRISM collected no data at the south pole.

Additional numerical details include the use of 16 streams for the discrete ordinates solution and aerosol phase functions are taken from [7,8].

Dust optical constants are from [7] and water ice optical constants were from [9].

Results: The τ_d results for CRISM EPF and the corresponding MARCI τ_{ice} retrievals from Mars Year 28/29/30 (2006-2011) are shown in Figure 2-3.

Dust opacity: We reported in [1] that the results for this period are consistent with background dust opacities of $\tau_d=0.3-0.5$ for the south polar region, with average excursions to 1.4 during the MY28 dust event. An updated retrieval model suggests that our estimates were low, although comparing Figure 3 with Figure 2 of [1] shows that the corrected peaks are scaled up in opacity (by a factor of 2), but identical in shape.

Dust Interpole Interannual Comparison: The CRISM EPF dataset south polar dust activity is far more pronounced and repeatable than the north polar data. We are still investigating potential bias in our dataset, but first glance the south pole dust activity is more sharply concentrated each year around $L_s=270$

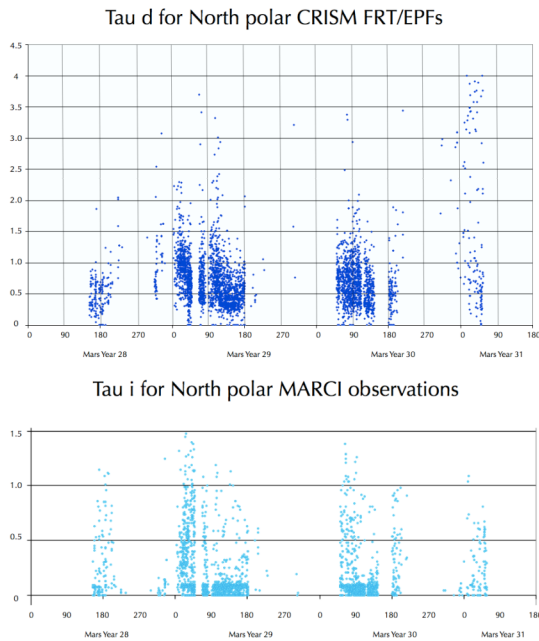


Figure 2. North polar τ_d and τ_i estimates for CRISM EPF/MARCI observations (poleward of 55°N) for MY28-30.

(southern vernal equinox). The north pole has a similar peak at $L_s=90$ (northern vernal equinox). MY28 was considerably more dusty than MY29 and 30 in both poles.

Water ice opacity: It should be noted that the MARCI retrievals presented here are only those corresponding to the CRISM EPF data – more complete MARCI analysis will be available at the time of the conference. Nevertheless, there does appear to be a peak in water ice opacity in due to the polar hood that reaches similar opacities (our model suggests peaks of $\tau_{ice}=1.5$) in each pole that diminishes gradually during springtime. Background water ice is much lower than background dust opacity for both poles (consistently in ‘background’ measurements, $\tau_{ice} < 0.1 < \tau_d$).

Conclusions: We have presented estimates of dust opacity from CRISM and ice cloud opacity from MARCI in the north (Figure 2) and south pole (Figure 3) for the first three Mars years of MRO operations (MY28-30), which included a large dust event at MY28/ $L_s=260-270$ and a smaller dust event in MY29 at the same time period. Future work will involve further investigations into MARCI water ice opacities throughout the year, filling in the gaps in our current observations.

Acknowledgements: Our thanks to Scott Murchie (CRISM PI) and the CRISM science operations team at JHU APL for their dedication to the task of obtain-

ing this unique dataset. Our thanks to Mike Smith for providing his cook files for Martian CO_2 profiles.

References: [1] Brown, A.J. and Wolff (2009) *LPSC XXIX* #1675 [2] Brown, A. et al. (2008) *LPSC XXIX* #2140 [3] Brown, A.J. et al., (2009) *JGR* 115, E00D13 doi:10.1029/2009JE003333 [4] Brown, A.J. et al. (2012) *JGR* 117, doi:10.1029/2012JE004113 [5] Murchie, S. et al. (2007) *JGR* 112 [6] Stamnes, K. et al. (1988) *AO* 27, [7] Wolff, M. et al. (2009) *JGR* doi:10.1029/2009JR003350 [8] Wolff, M. et al. (2011) *4th International Wksp on the Mars Atmosphere*, Paris p. 213-216 [9] Warren, S.G. (1984) *AO* 23, 1206-1225

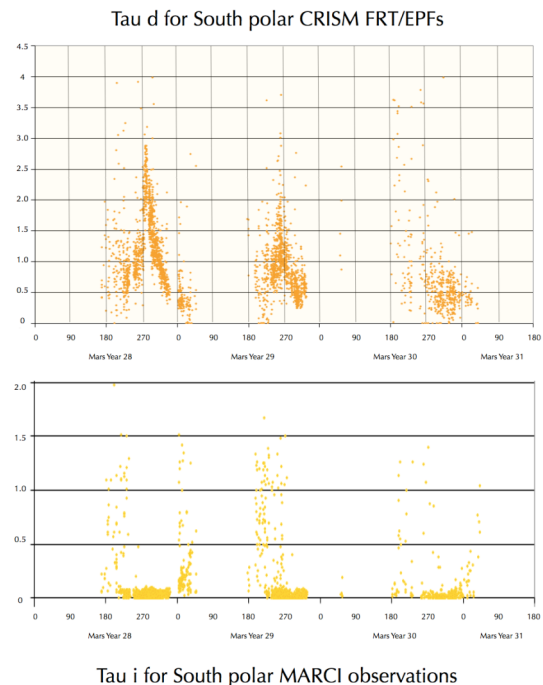


Figure 3. South polar τ_d and τ_i estimates for CRISM EPF/MARCI observations (poleward of 55°S) for MY28-30.